

CHAPTER IV

RESULTS AND DISCUSSION

4.1 Effect of Amphiphile Concentration

The effect of the concentration of amphiphiles using DBSA and NP on the rate of asphaltene dissolution was carried out for both of fraction 1 and fraction 2 in heptane as alkane media.

Figure 4.1 shows the time - evolution profile of asphaltene fraction 1 dissolution as a function of the DBSA - concentration. It is clear that the rate of dissolution increases with the increasing of DBSA concentration. However, the rate of dissolution increases slightly from DBSA concentration 7.5 wt % to 10 wt%. This trend also shows with asphaltene fraction 2 in Figure 4.2 where the increment in the rate of asphaltene dissolution with increasing DBSA concentration from 5.0 wt% to 10.0 wt % is quite small.

Figure 4.3 shows the time - evolution profile of asphaltene fraction 1 as a function of NP concentration. The result shows the significantly increasing of the rate of asphaltene dissolution when increasing the NP concentration from 5 wt% to 20 wt% . The minimum NP concentration in order to completely dissolve the asphaltene fraction 1 deposit is 20 wt%. However, Figure 4.4 shows that to completely dissolve asphaltene fraction 2, it is required the NP concentration only 10 wt%.

It is noted that there is a difference in the minimum amphiphile concentrations required to completely dissolve asphaltene deposits in both fractions. That is, for asphaltene fraction 1, it is required 2.5 wt% of DBSA and 20 wt% of NP solutions while it is required 2.5 wt% of DBSA and 10 wt%

of NP solution for asphaltene fraction 2. Because of the strength of DBSA - asphaltene associations being much higher than the NP- asphaltene associations (Chang and Fogler, 1994), the low DBSA concentration is sufficient for stabilizing asphaltene in the solutions. The minimum NP concentrations for asphaltene fraction 1 is higher than that for asphaltene fraction 2. It indicates that the asphaltene fraction 1 comprises of the functional groups with degree of polarity being higher than that in asphaltene fraction 2. Hence, the asphaltene fraction 1 can only be dissolved completely in the solution with higher NP concentration.

The data in Figures 4.1 - 4.4 were replotted in Figures 4.5 - 4.8 in term of the logarithm of undissolved asphaltene mass fraction ($\log M/M_0$) - versus - time. The specific dissolution rate constants, k , were calculated from the slope of linear fitting between $\ln (M/M_0)$ - versus - time. And they were plotted as a function of amphiphile concentrations in Figures 4.9 - 4.10. Figure 4.9 shows that the k - values for asphaltene fraction 1 and fraction 2 increase steadily at low DBSA concentration and level off at high DBSA concentration. The k -values are constant at about 0.12 min^{-1} and 0.22 min^{-1} for asphaltene fraction 1 and fraction 2 respectively when the concentration of DBSA in heptane reaches 0.5 M. Figure 4.10 shows that the k - values for asphaltene fraction 1 increase significantly until the NP concentration reaches 0.65 M. The k - values for asphaltene fraction 2 increase steadily at below 1.2 M of NP concentration. When the NP concentration reaches 1.2 M, the k -values level off at 0.17 min^{-1} . Except the asphaltene fraction 1 / NP system, the others show the same trend in increasing of k - values at low amphiphile concentration and level off at some higher amphiphile concentration. These trends suggest that the variation of k - value with respect to the amphiphile concentration can be described by a Langmuir - Hinshelwood kinetics from the asphaltene dissolution model.

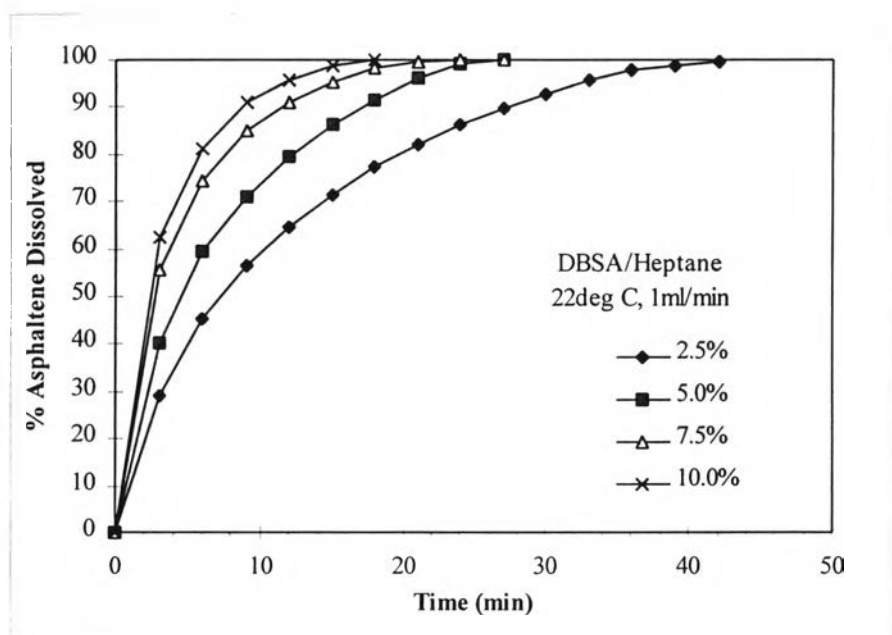


Figure 4.1 The profile of asphaltene fraction 1 dissolution by heptane-based fluid containing different concentrations of DBSA amphiphile.

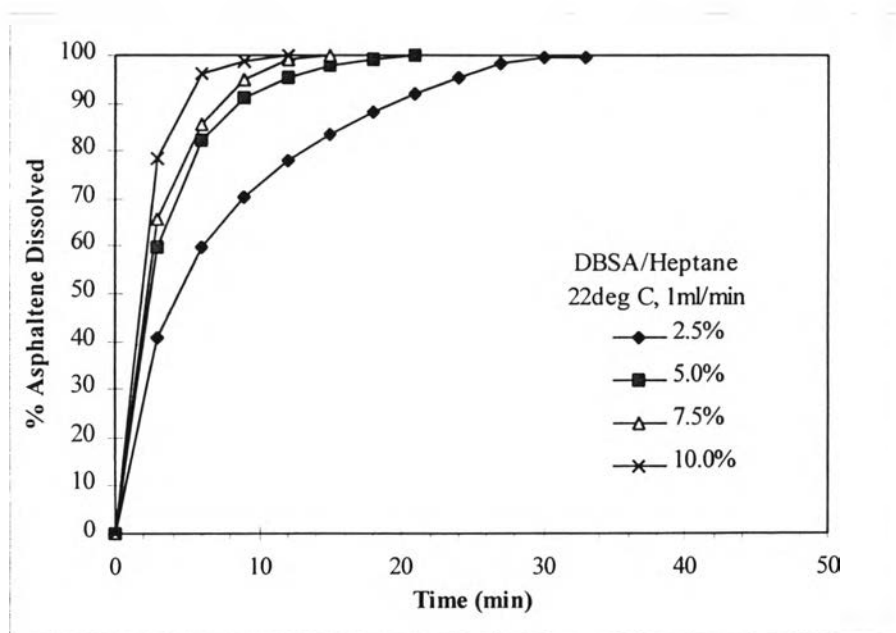


Figure 4.2 The profile of asphaltene fraction 2 dissolution by heptane-based fluid containing different concentrations of DBSA amphiphile.

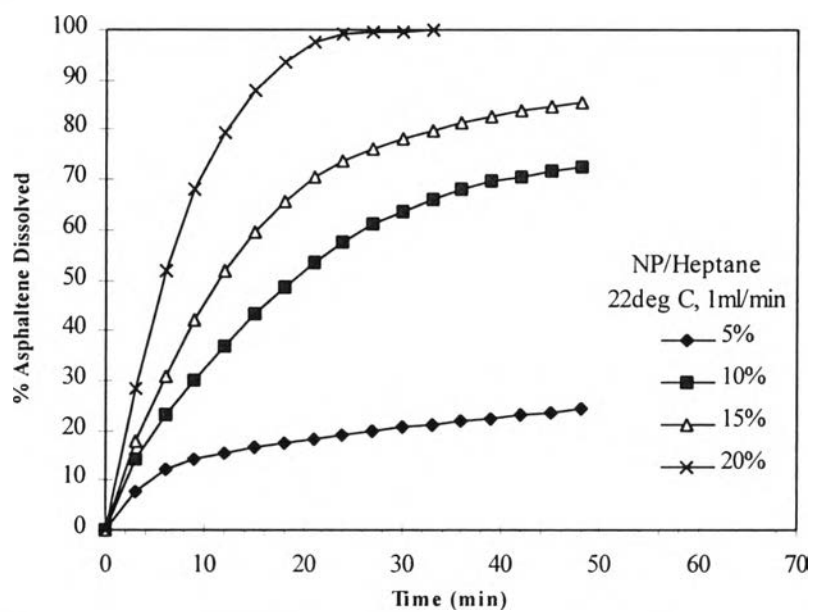


Figure 4.3 The profile of asphaltene fraction 1 dissolution by heptane-based fluid containing different concentrations of NP amphiphile.

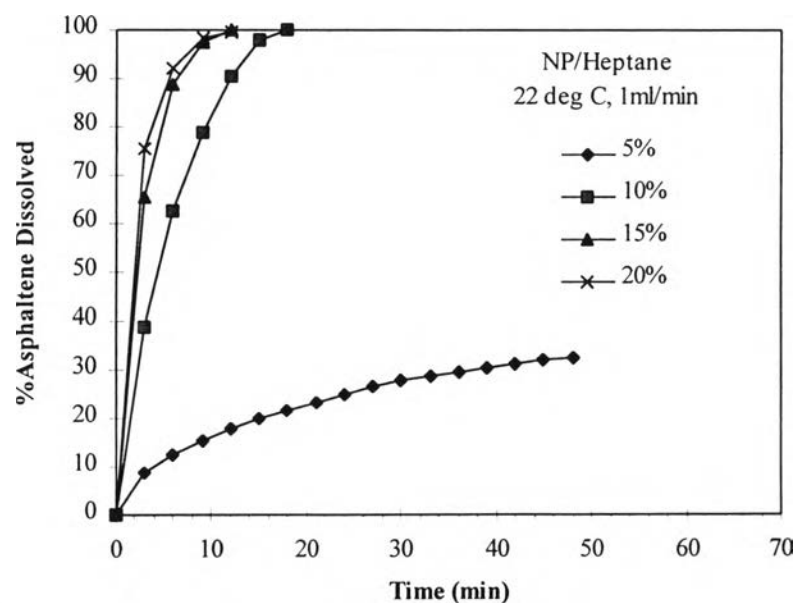


Figure 4.4 The profile of asphaltene fraction 2 dissolution by heptane-based fluid containing different concentrations of NP amphiphile.

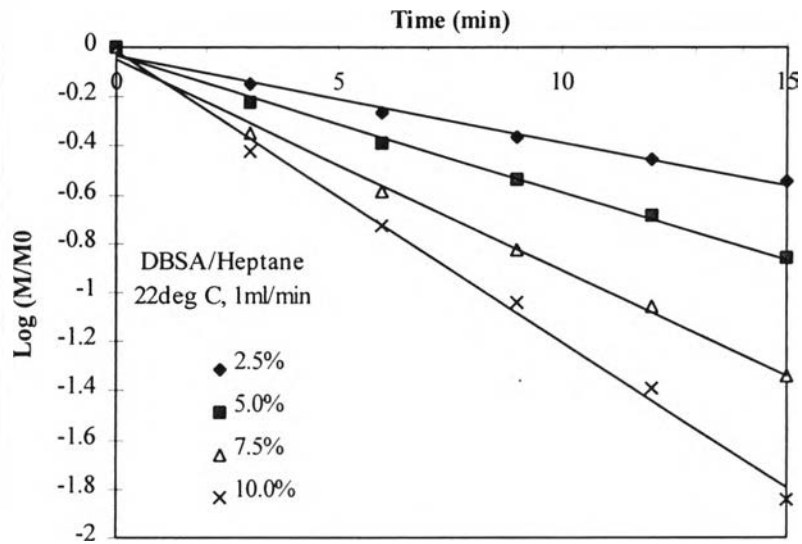


Figure 4.5 Kinetic analysis of asphaltene fraction 1 dissolution by heptane-based fluid containing different concentrations of DBSA amphiphile.

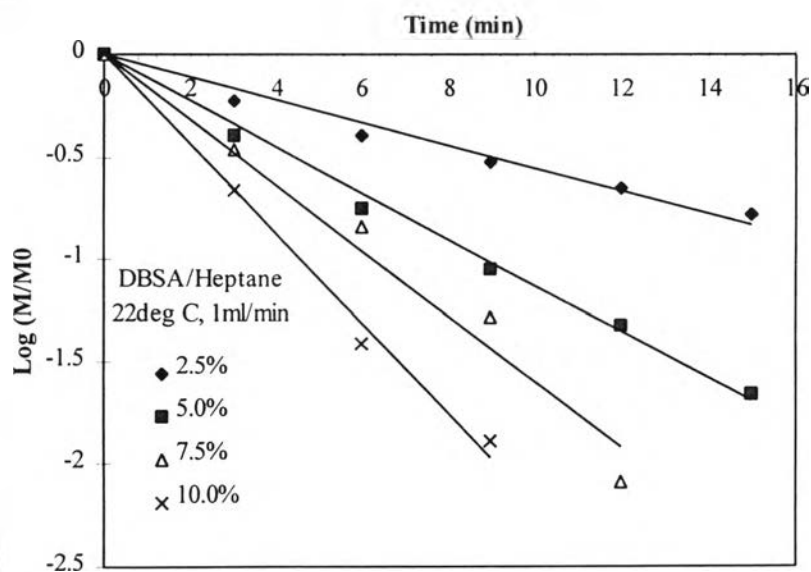


Figure 4.6 Kinetic analysis of asphaltene fraction 2 dissolution by heptane-based fluid containing different concentrations of DBSA amphiphile.

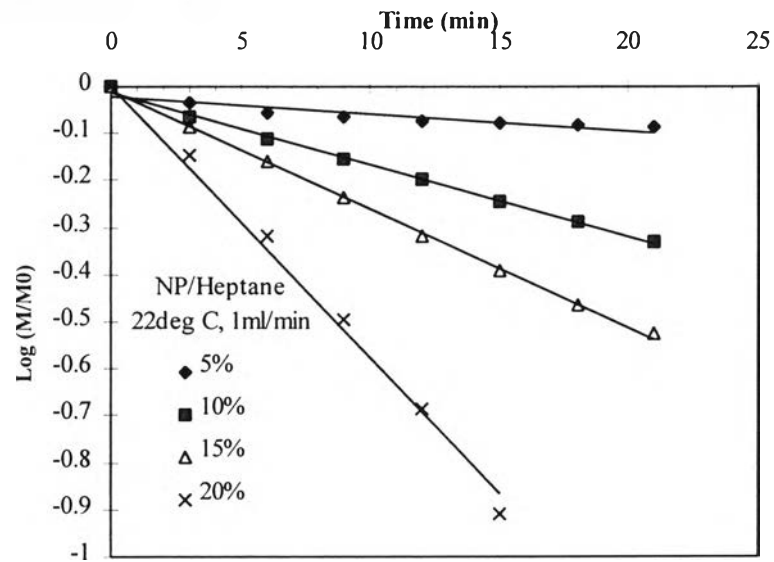


Figure 4.7 Kinetic analysis of asphaltene fraction 1 dissolution by heptane-based fluid containing different concentrations of NP amphiphile.

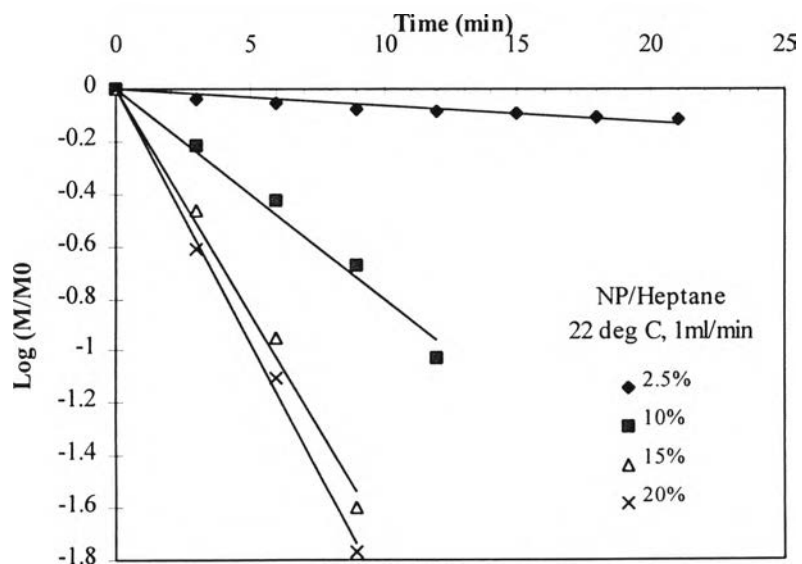


Figure 4.8 Kinetic analysis of asphaltene fraction 2 dissolution by heptane-based fluid containing different concentrations of NP amphiphile.

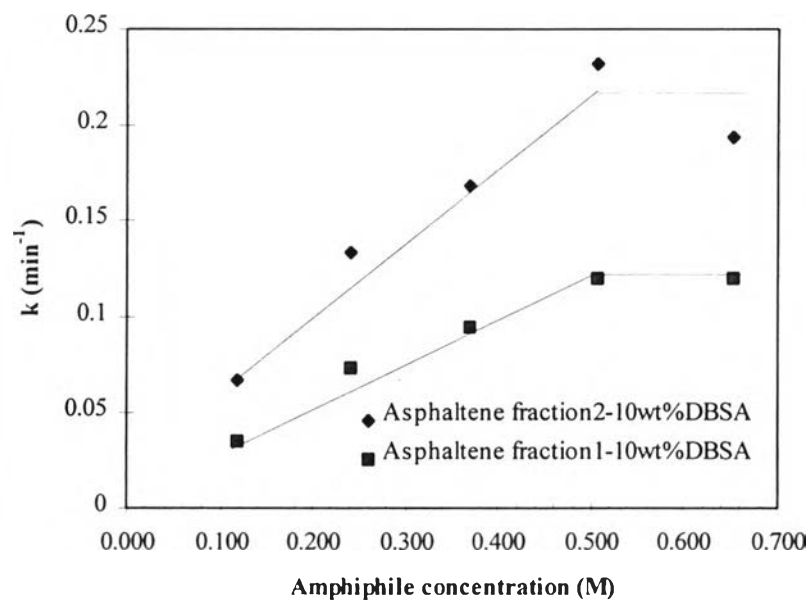


Figure 4.9 The specific dissolution rate constant, k , as a function of the DBSA concentration in solutions.

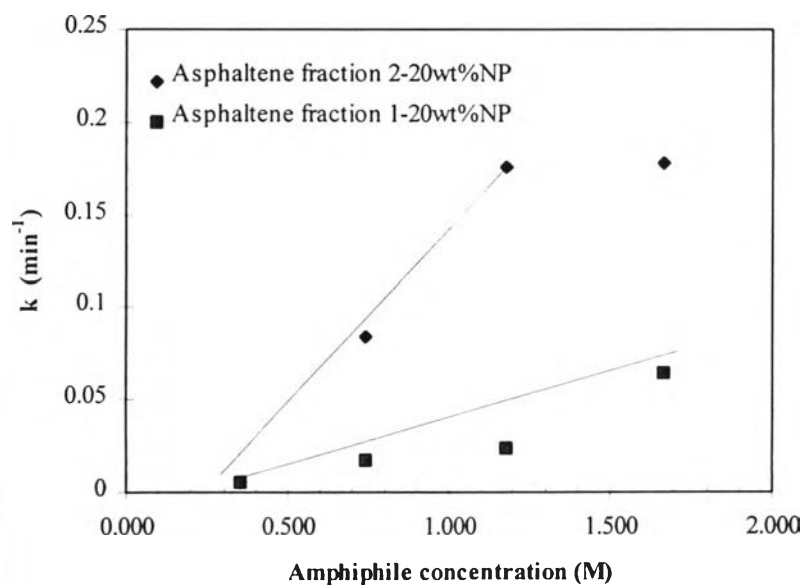
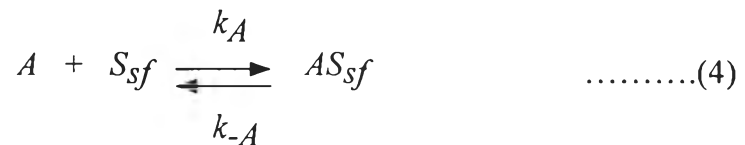


Figure 4.10 The specific dissolution rate constant, k , as a function of the NP concentration in solutions.

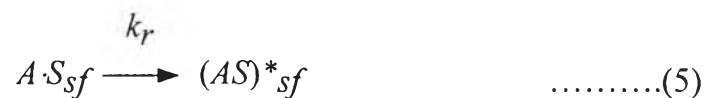
The dissolution of asphaltene precipitates in amphiphile / alkane solution involves both mass transfer and surface reaction processes. As shown in Figure 4.11, the dissolution of asphaltene involve the following step (Fogler, 1992). The amphiphile is first transported from the bulk liquid to the asphaltene surface.



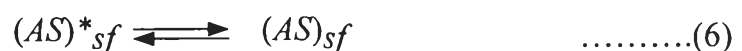
Where S_{bk} and S_{sf} are amphiphiles in the bulk fluid and at the asphaltene surfaces, respectively. Subsequently, the amphiphile near asphaltene adsorbs on the functional site - on the asphaltene surfaces.



to form the amphiphile - asphaltene complex



This step is called the surface reaction step. "A" represents the functional sites on the asphaltene surface on which the amphiphile can adsorb. Afterwards, the amphiphile- asphaltene complex desorbs from the asphaltene surface.



and is transported to the bulk liquid



where $(AS)_{sf}$ and $(AS)_{bk}$ are the asphaltene - amphiphile associated complex on the asphaltene surface and in the bulk fluid, respectively.

At equilibrium, the net rate of adsorption equals zero, hence

$$[A \cdot S_{sf}] = K_A [A][S_{sf}] \quad \dots\dots\dots(8)$$

where $K_A = k_A / k_{-A}$. With the first order model, the total number of functional sites on asphaltene surfaces is assumed to be proportion to the mass of undissolved asphaltenes and is the sum of the bound and unbound sites. That is,

$$\begin{aligned} M &= [A] + [(AS)_{sf}] = [A] + K_A [A][S_{sf}] \\ [A] &= \frac{M}{1 + K_A [S_{sf}]} \quad \dots\dots\dots(9) \end{aligned}$$

Then, the rate of asphaltene dissolution becomes

$$-\frac{dM}{dt} = k_r [A \cdot S_{sf}] = k_r K_A [A][S_{sf}] = k_r K_A \frac{M[S_{sf}]}{1 + K_A [S_{sf}]} \quad \dots\dots\dots(10)$$

which is a Langmuir - Hinshelwood form as the observed experimentally in Figure 4.9 - 4.10. At low amphiphile concentration, the rate of the amount of amphiphile adsorbing on asphaltene increases linearly with increasing the concentration of amphiphile ; hence the rate of asphaltene dissolution increases

with the increasing of amphiphile concentration correspondingly. At sufficient high amphiphile, most functional group of hydrogen bonding or charge transfer interactions on asphaltene surfaces are already bonded with amphiphiles .

Therefore, the rate of asphaltene dissolution cannot further increase with further increasing amphiphile concentration. However, the k - variation of asphaltene fraction 1 in NP, which is steadily increasing with the increase of amphiphile concentration, indicates that the amount of NP molecules in the 20 wt% NP may not be enough to bound with all of functional groups on asphaltene surfaces. Since the high degree of polarity of asphaltene fraction 1 and the weak interactions between NP and asphaltenes, there are unbond sites left on the asphaltene fraction 1 surface. The rate of dissolution displays the trend to be increased with further increasing of NP concentration.

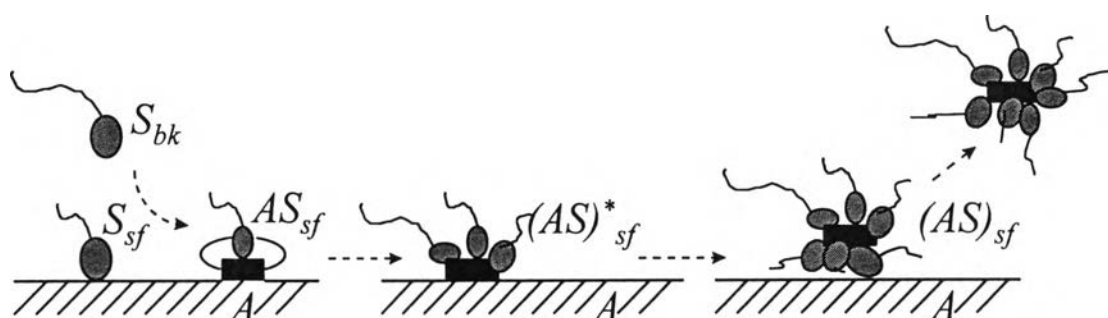


Figure 4.11 The process of the dissolution of asphaltene.

4.2 Effect of Flow Rate

Figures 4.12 - 4.15 show the effect of flow rates of amphiphile-alkane solution on the dissolution profiles for asphaltene fraction 1 in 10wt% DBSA (AspF1-10DBSA), asphaltene fraction 1 in 20wt% NP (AspF1-20NP), asphaltene fraction 2 in 10wt% DBSA (AspF2-10DBSA), and asphaltene fraction 2 in 20wt% NP (AspF2-20NP). The flow rate represents the character of fluid and contributes to the rate of asphaltene dissolution. The dissolution process of asphaltenes involves two significant steps, diffusion (i.e. mass transfer) and surface reactions step as mentioned earlier. The diffusion step, amphiphiles molecules are transferred from bulk fluid to asphaltenes surface. The rate of mass transfer for amphiphiles can be described as

$$-\frac{dM}{dt} = k_c \left[[S_{bk}] - [S_{sf}] \right] \quad \dots\dots\dots(11)$$

The surface reactions occur by the amphiphiles adsorbing on the asphaltene surface. Then the product of amphiphiles bonded with asphaltene molecules are transferred to bulk liquid. The rate of mass transfer for dissolved asphaltene is described as

$$-\frac{dM}{dt} = k_c \left[[AS_{sf}] - [AS]_{,sk} \right] \quad \dots\dots\dots(12)$$

By describing the dissolution process of asphaltene, the flow rate of amphiphile/alkane solution can be considered to be the function of mass transfer coefficient (k_c).

$$k_c = 0.6 \left(\frac{D_s^{2/3}}{\nu^{1/6}} \right) \left(\frac{U^{1/2}}{d_p^{1/2}} \right) \quad \dots\dots(13)$$

where D_s is diffusivity of reaching species. ν is the kinematic viscosity. d_p is the sizes of asphaltene precipitates and U is fluid velocity.

Since the flow rate equals to the product of the cross-sectional area of the reactor and fluid velocity, then

$$F = U \times A \quad \dots\dots(14)$$

$$F \propto U \quad \dots\dots(15)$$

Therefore, the relation between flow rate and mass transfer coefficient is

$$k_c = BU^{1/2} \quad \dots\dots(16)$$

where B is constant

$$\log k_c = \log U + \log B \quad \dots\dots(17)$$

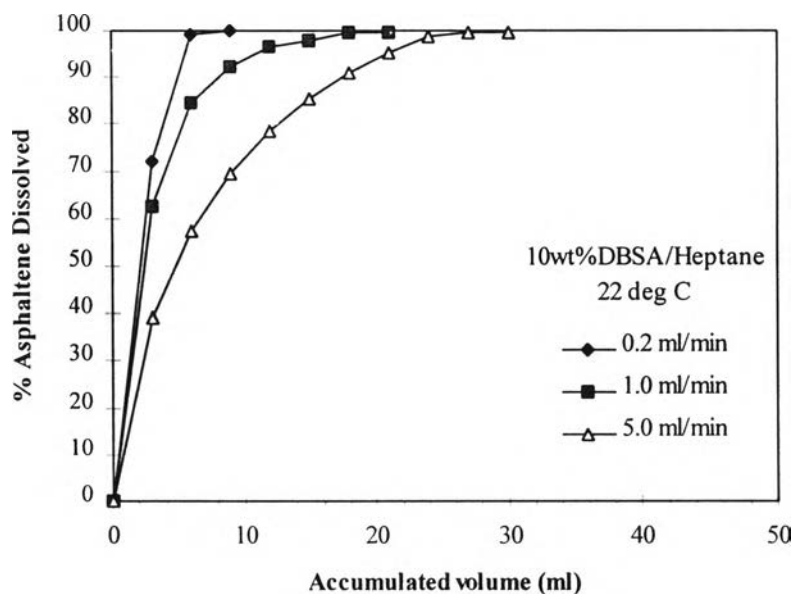


Figure 4.12 The profile of asphaltene fraction 1 dissolution by heptane-based fluid containing 10wt% DBSA amphiphile at different flow rates.

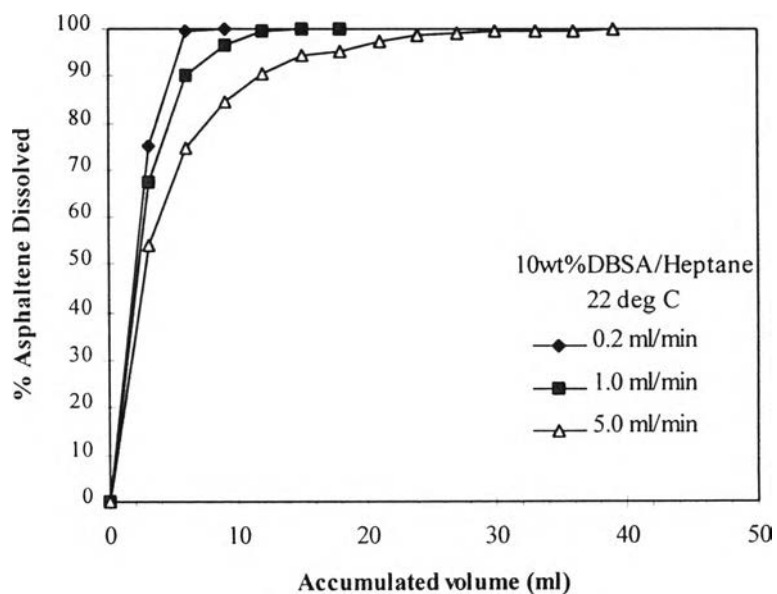


Figure 4.13 The profile of asphaltene fraction 2 dissolution by heptane-based fluid containing 10wt% DBSA amphiphile at different flow rates.

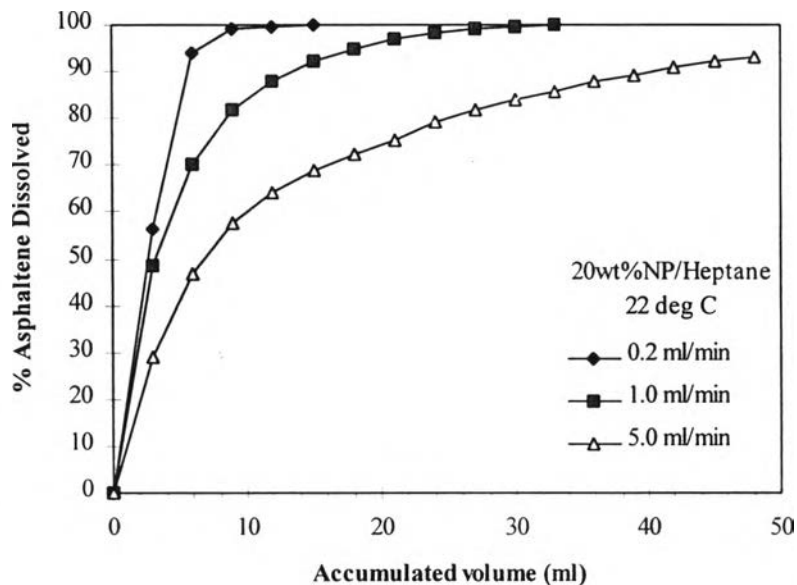


Figure 4.14 The profile of asphaltene fraction 1 dissolution by heptane-based fluid containing 20wt% NP amphiphile at different flow rates.

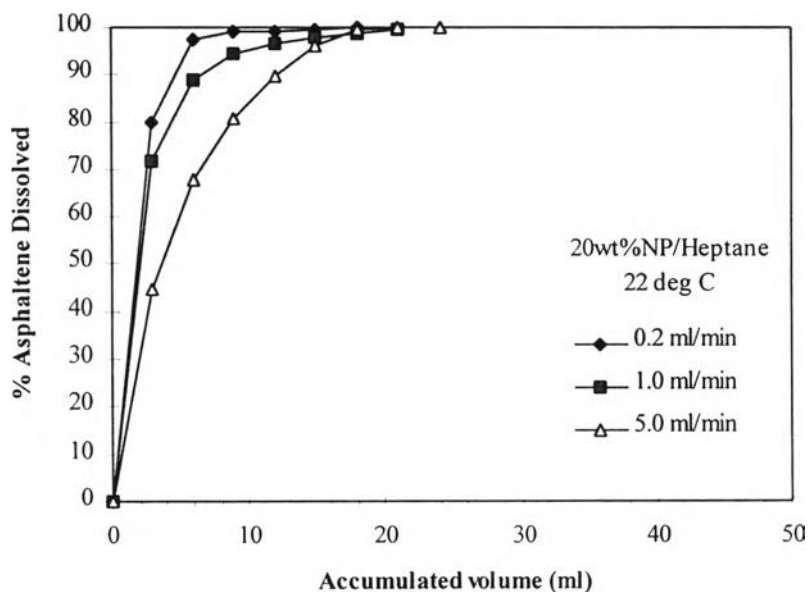


Figure 4.15 The profile of asphaltene fraction 2 dissolution by heptane-based fluid containing 20wt% NP amphiphile at different flow rates

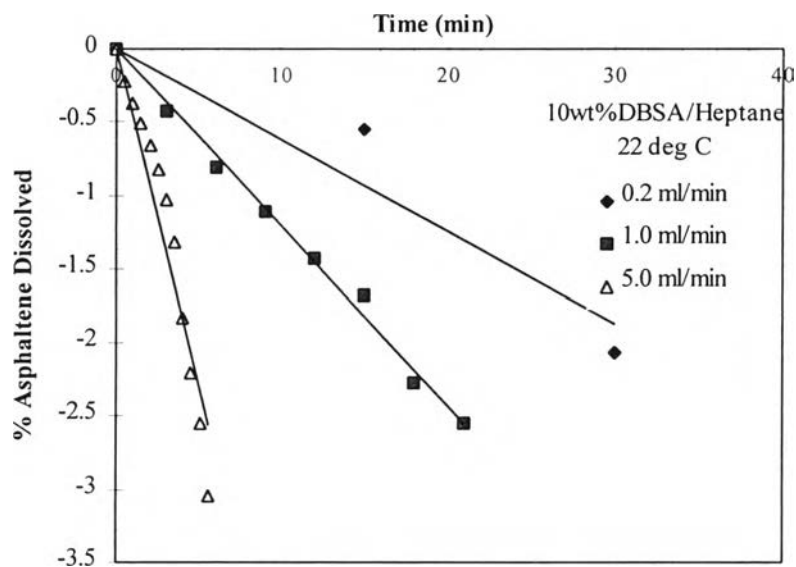


Figure 4.16 Kinetic analysis of asphaltene fraction 1 dissolution by heptane-based fluid containing 10wt% DBSA amphiphile at different flow rates.

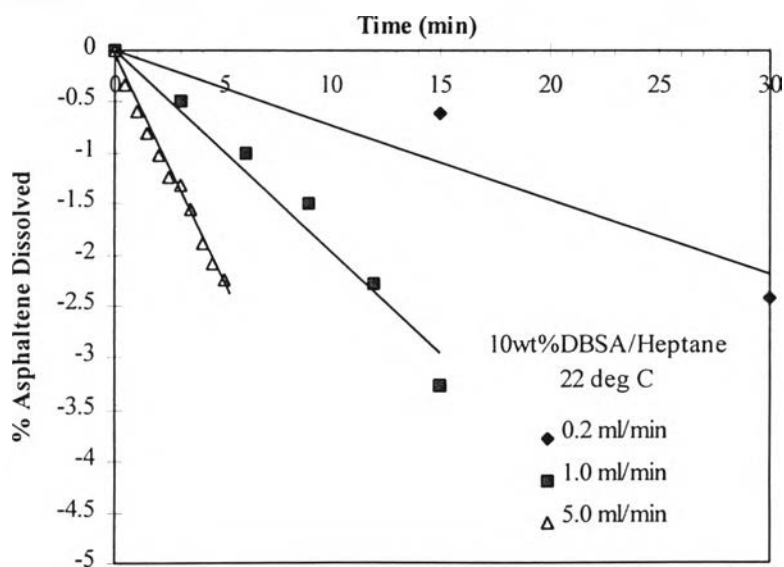


Figure 4.17 Kinetic analysis of asphaltene fraction 1 dissolution by heptane-based fluid containing 10wt% DBSA amphiphile at different flow rates.

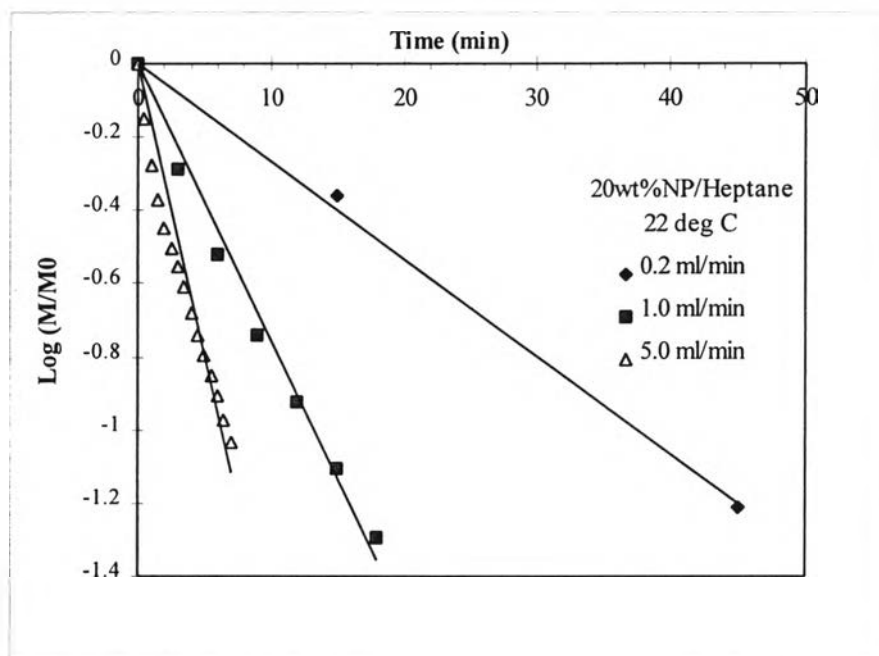


Figure 4.18 Kinetic analysis of asphaltene fraction 1 dissolution by heptane-based fluid containing 20wt% NP amphiphile at different flow rates.

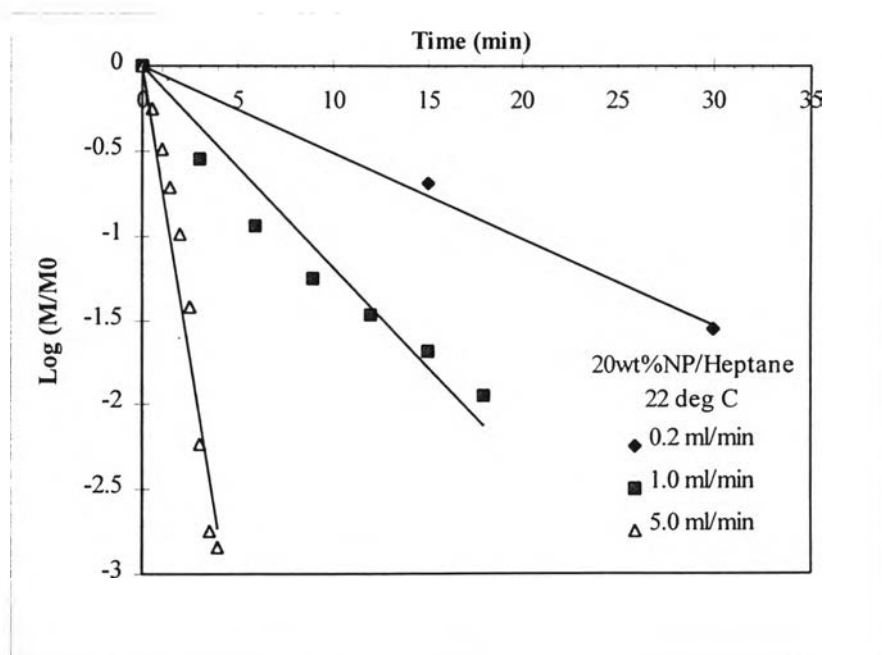


Figure 4.19 Kinetic analysis of asphaltene fraction 2 dissolution by heptane-based fluid containing 20wt% NP amphiphile at different flow rates.

The data in Figures 4.12 - 4.15 were replotted into Figures 4.16 - 4.19. The obtained specific rate constants were plotted in term of $\log k$ with $\log U$. The slope from the Figures 4.20 - 4.23 are summarized in Table 4.1. It is clear that the slope of the plot between $\log k$ and $\log U$ in the dissolution of AspF1-10DBSA, AspF1-20NP and AspF2-20NP are close to 0.5. It indicates that these systems are dominated by the mass transfer process. This can be explained that DBSA, which is the amphiphile with acidic head groups, can readily donate the protons to $c=c$ bonds and/or basic portions in asphaltene surfaces. It results that the DBSA-asphaltene association becomes the strong acid-base interaction and the irreversible attraction interactions with asphaltene (Chang and Fogler, 1993&1994). Hence, DBSA can adsorb on the asphaltene surface rapidly through the acidic head group even on the surface with high degree of polarity of asphaltene fraction 1. Therefore, these systems have the fast surface reaction and the diffusion is the rate-limiting step. However, since the slope of the dissolution of AspF1-20NP is far from 0.5, it indicates that the system is hardly limited by the mass transfer. The NP-asphaltene association is the hydrogen bonding and belongs to a weak acid-base interaction. Therefore, to stabilize the asphaltene fraction 1 in the solution, it is required the high NP concentration. Hence, the system undergoes the fast diffusion of NP molecules in order to provide the sufficient NP molecules on the asphaltene fraction 1 surfaces and accomplish the surface reactions. Therefore, the dissolution of AspF1-20NP may be limited by the surface reaction step.

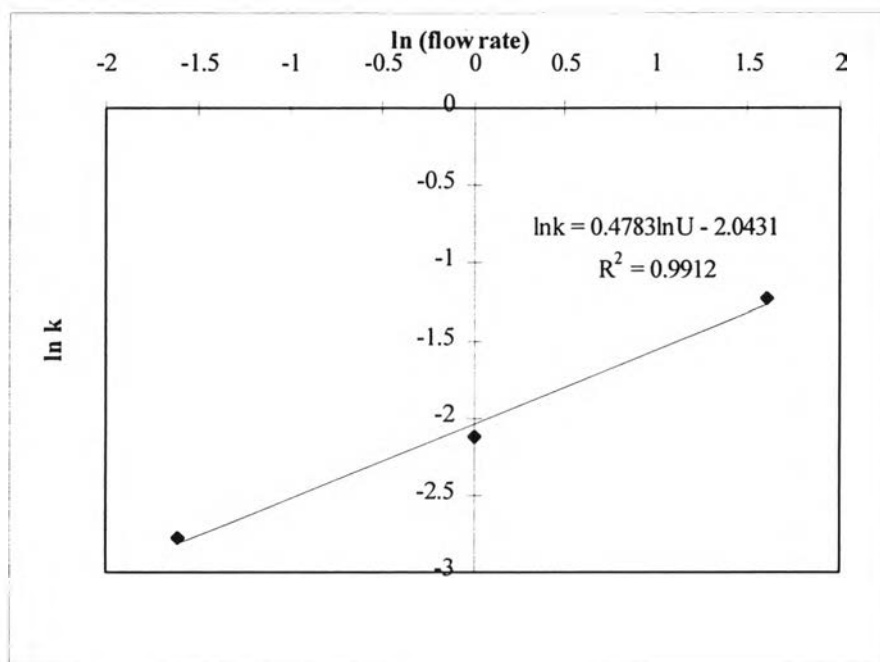


Figure 4.20 The specific dissolution rate constant, k of asphaltene fraction 1 as a function of the 10wt% DBSA-heptane solution flow rate.

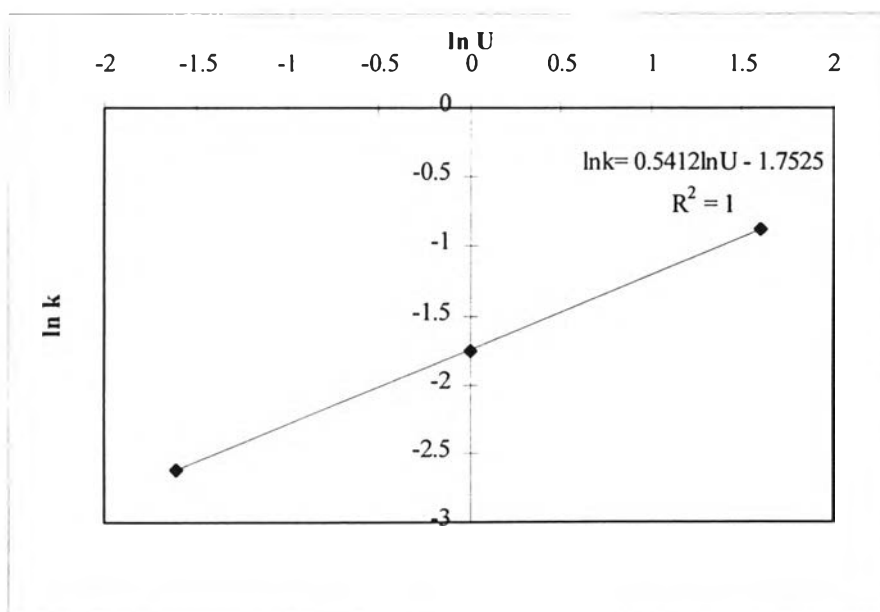


Figure 4.21 The specific dissolution rate constant, k of asphaltene fraction 2 as a function of the 10wt% DBSA-heptane solution flow rate.

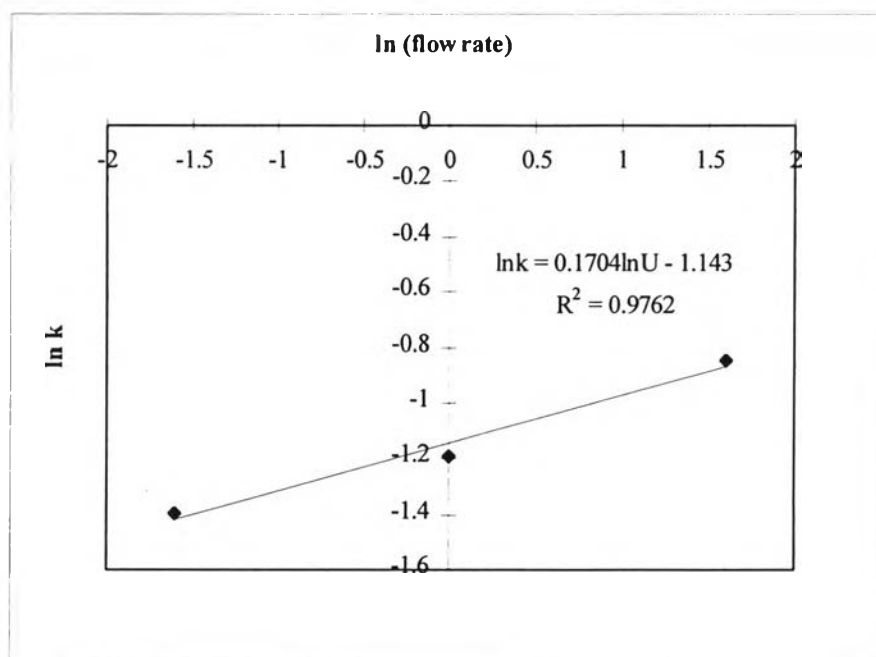


Figure 4.22 The specific dissolution rate constant, k of asphaltene fraction 1 as a function of the 20wt% NP-heptane solution flow rate.

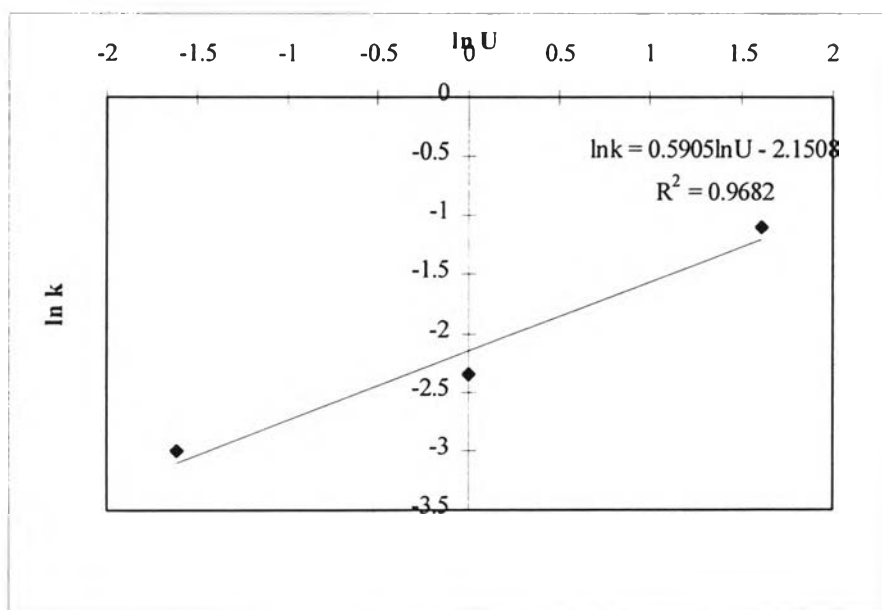


Figure 4.23 The specific dissolution rate constant, k of asphaltene fraction 2 as a function of the 20wt% NP-heptane solution flow rate.

Table 4.1 The slope of the relation between logarithm of specific dissolution rate constant and flow rate at each of fractionated asphaltene in amphiphile – heptane solutions

Fractionated Asphaltenes- Amphiphile/Heptane solution	The slope of the relation
AspF1-10DBSA	0.4783
AspF1-20NP	0.5412
AspF2-10DBSA	0.1704
AspF2-20NP	0.5905

4.3 Effect of Temperature

The effect of temperature on the rate of asphaltene dissolution was investigated by performing the experiment for 3 temperatures: 10°C, 22 °C, and 58°C. Figures 4.24 - 4.27 illustrate the dissolution profiles for AspF1-10DBSA, AspF1-20NP, AspF2-10DBSA, AspF2-20NP, respectively.

The results show that the rate of asphaltene dissolution increases with the increasing of fluid temperature as shown in Figures 4.28 - 4.31.

With arrhenius equation, the specific rate constants are also obtained from the slope of linear fitting curve in Figures 4.32 - 4.35.

$$K = A \exp\left(-\frac{E_a}{RT}\right) \quad \dots\dots\dots(18)$$

where A is the pre-experimental constant, R is 1.987 cal/mole K, ideal gas constant and E_a is the activation energy.

Since the experimental data are linearly fitted well, the activation energies (E_a) were calculated from the slope fitting data points. Figure 4.36 shows the value of activation energy for each system which are 5.87, 2.41, 10.77, and 4.11 kcal/mole for AspF1-10DBSA, AspF1-20NP, AspF2-10DBSA, AspF2-20NP, respectively.

The E_a of AspF1-10DBSA is higher than that of AspF1-20NP. It is also the other evidence that the asphaltene-asphaltene associations in fraction 1 are stronger than that in fraction 2. Therefore, it is required the higher energy for fraction 1 to break the aggregated bonding and to proceed the dissolution process. The E_a values of AspF1-10DBSA and AspF2-10DBSA are less than the E_a values of AspF1-20NP and AspF2-20NP. The fact supports the idea that the DBSA-asphaltene associations are stronger than the NP-asphaltene associations. Therefore asphaltene fraction 1 requires less energy than fraction 2 for stabilizing asphaltene in the solution. Since the obtained E_a values are corresponding with the typical energy value of intermolecular hydrogen bonding (in the range of 3-7 kcal/mole) and charge transfer associations (generally less than 8 kcal/mole) that may occur between asphaltene molecules, e.g. phenol (Pimental and McClellan, 1960 ; Sliken, 1971 ; Barbour and Peterson, 1974). Hence, increasing of fluid temperature enhances the rate of asphaltene dissolution through the reactions on the surface of asphaltene which involve the transition from asphaltene-asphaltene associations to

asphaltene-amphiphile associations via the redistribution of inter-molecular hydrogen bonding and charge transfer interactions. In addition, the mass transfer of asphaltene and amphiphile in the dissolution process may also be a cause of the temperature-dependent asphaltene dissolution rate. Since at higher temperature, the fluid has larger diffusivities that can undergo the higher molecular collisions which contribute to the higher rate of asphaltene dissolution.

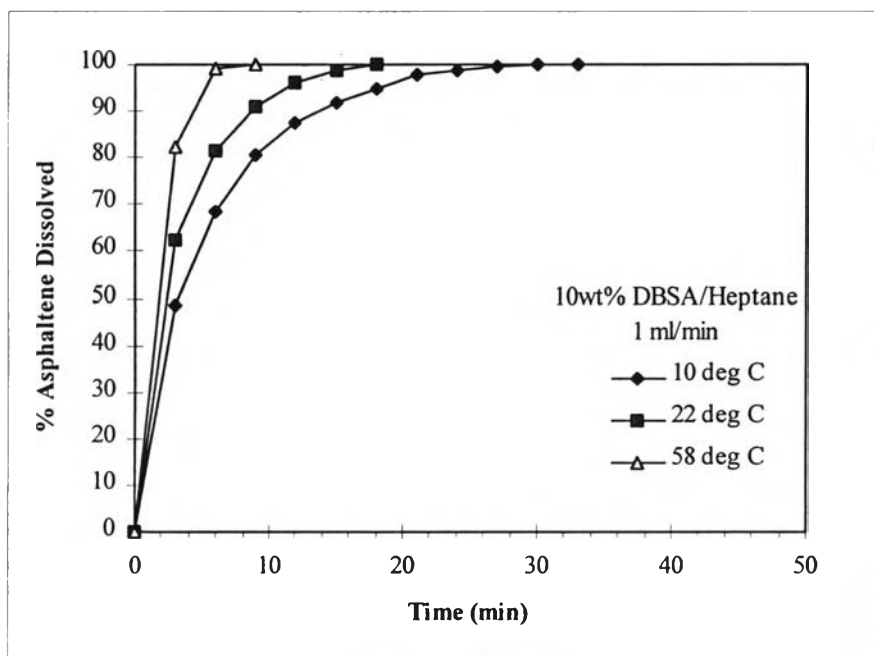


Figure 4.24 The profile of asphaltene fraction 1 dissolution by heptane-based fluid containing 10wt% DBSA amphiphile at different temperatures.

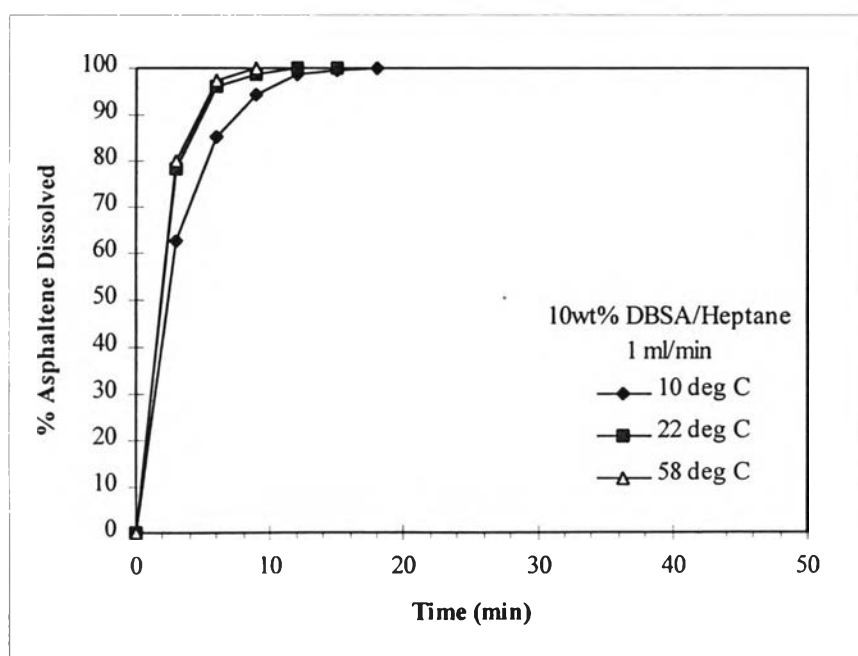


Figure 4.25 The profile of asphaltene fraction 2 dissolution by heptane-based fluid containing 10wt% DBSA amphiphile at different temperatures.

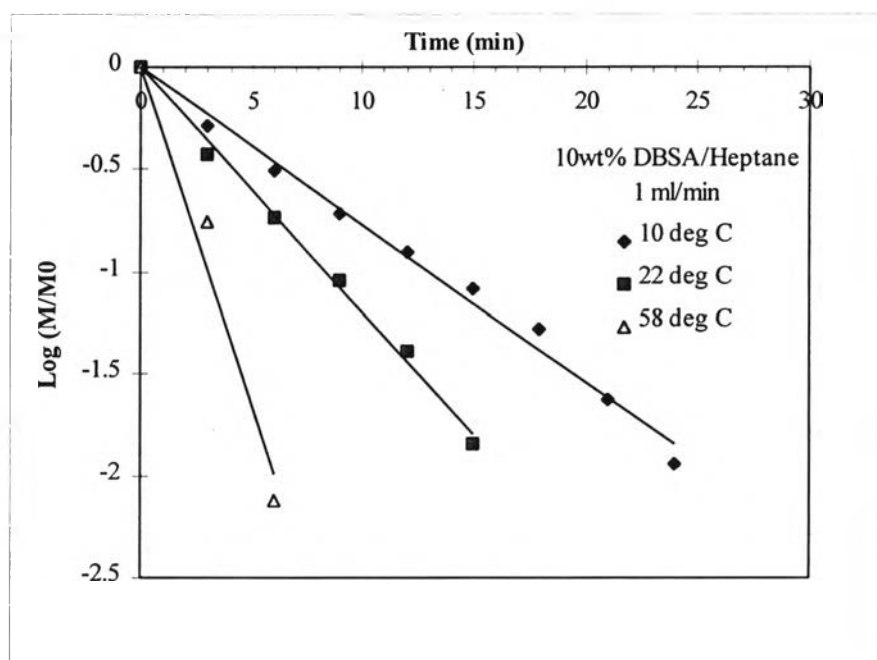


Figure 4.26 Kinetic analysis of asphaltene fraction 1 dissolution by heptane-based fluid containing 10wt% DBSA amphiphile at different temperatures.

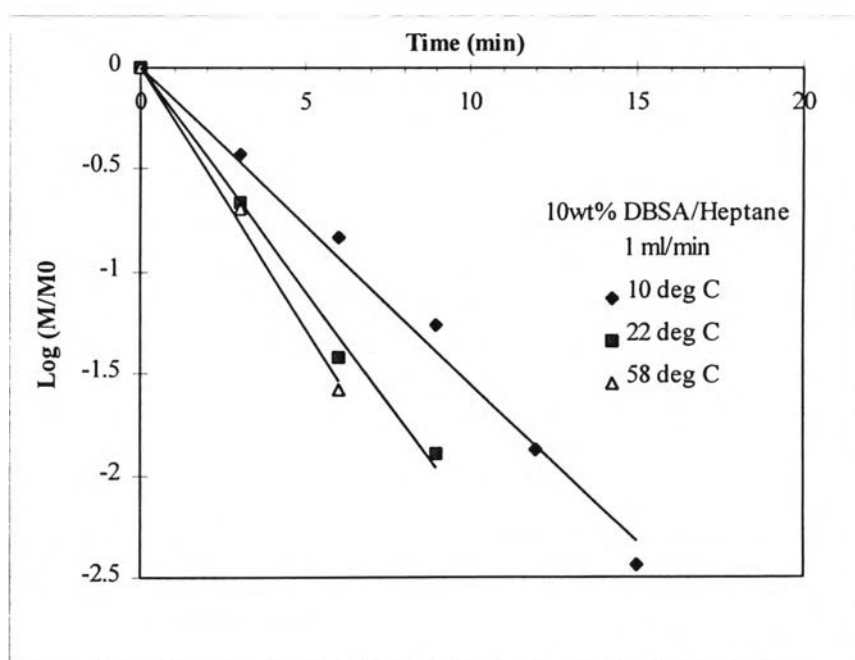


Figure 4.27 Kinetic analysis of asphaltene fraction 2 dissolution by heptane-based fluid containing 10wt% DBSA amphiphile at different temperatures.

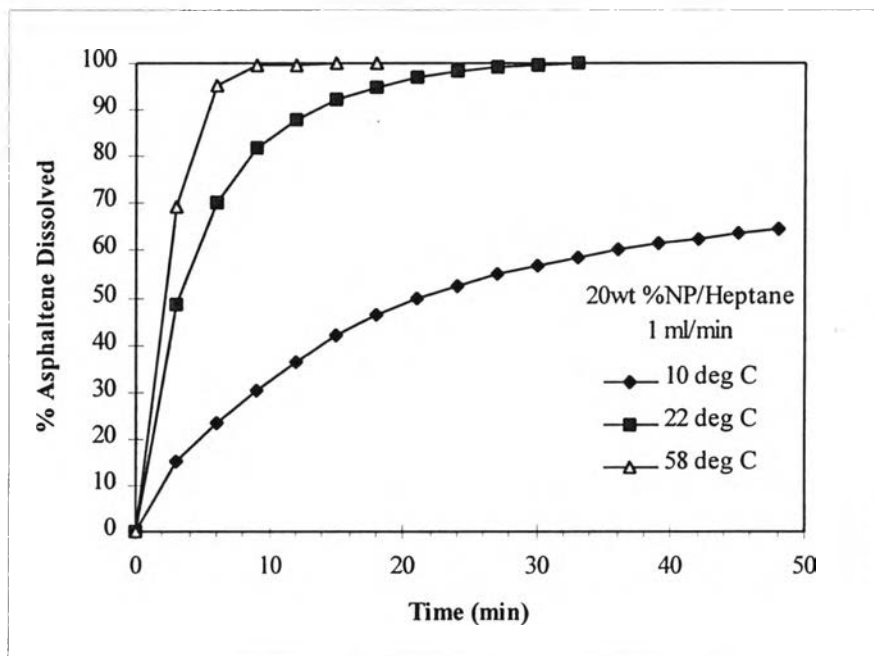


Figure 4.28 The profile of asphaltene fraction 1 dissolution by heptane-based fluid containing 20wt% NP amphiphile at different temperatures.

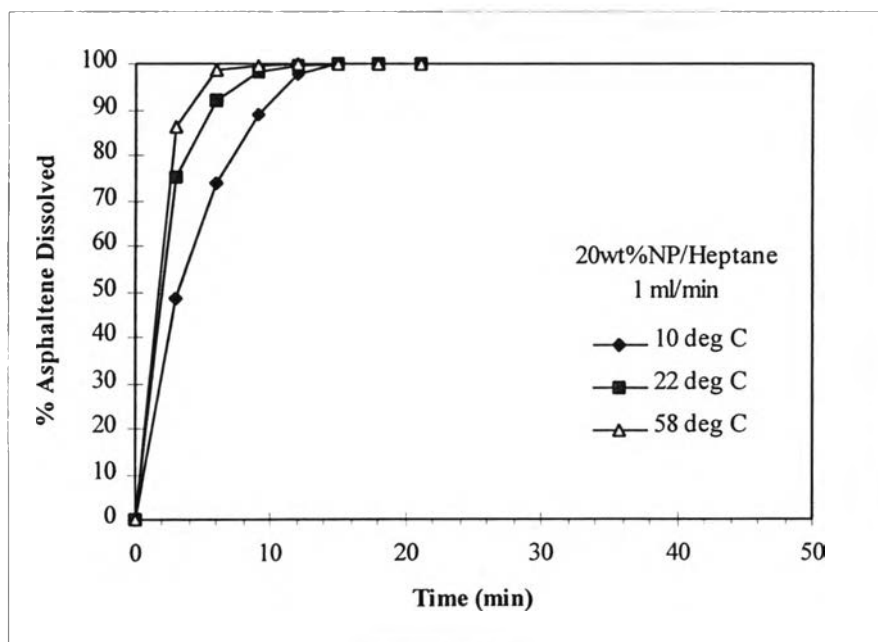


Figure 4.29 The profile of asphaltene fraction 2 dissolution by heptane-based fluid containing 20wt% NP amphiphile at different temperatures.

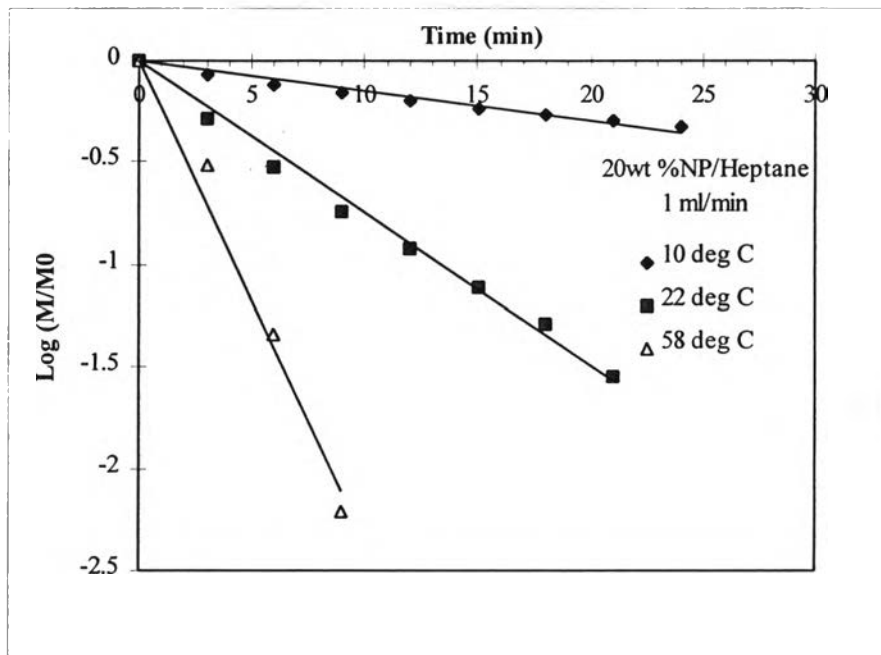


Figure 4.30 Kinetic analysis of asphaltene fraction 1 dissolution by heptane-based fluid containing 20wt% NP amphiphile at different temperatures.

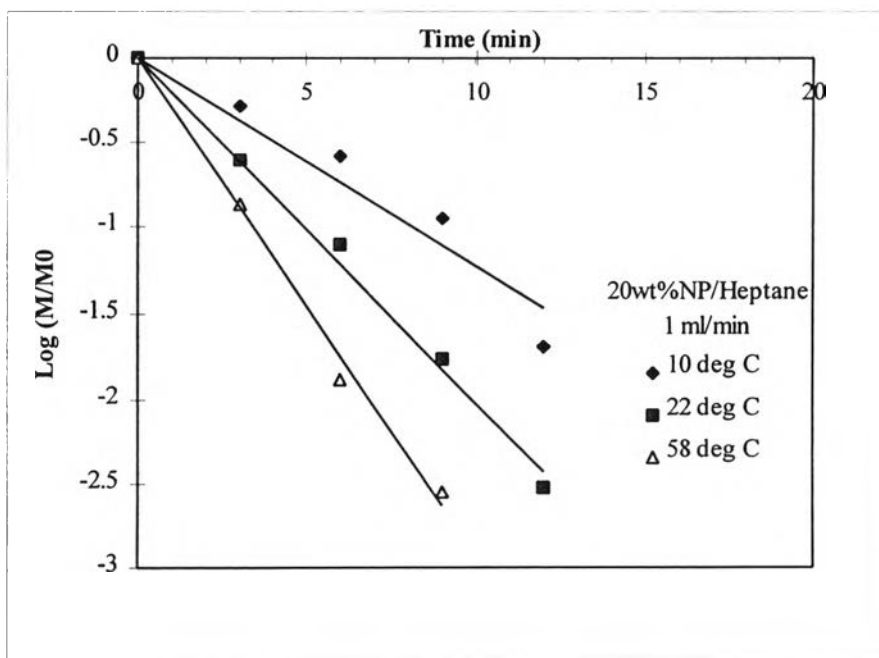


Figure 4.31 Kinetic analysis of asphaltene fraction 2 dissolution by heptane-based fluid containing 20wt% NP amphiphile at different temperatures.

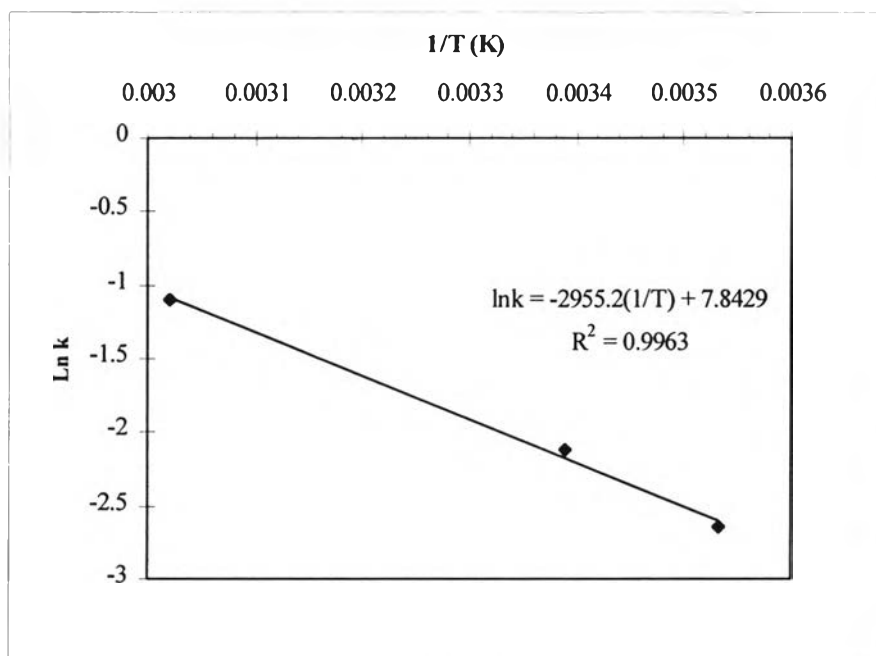


Figure 4.32 The specific dissolution rate constant, k , of asphaltene fraction 1 as a function of the 10wt% DBSA-heptane temperature.

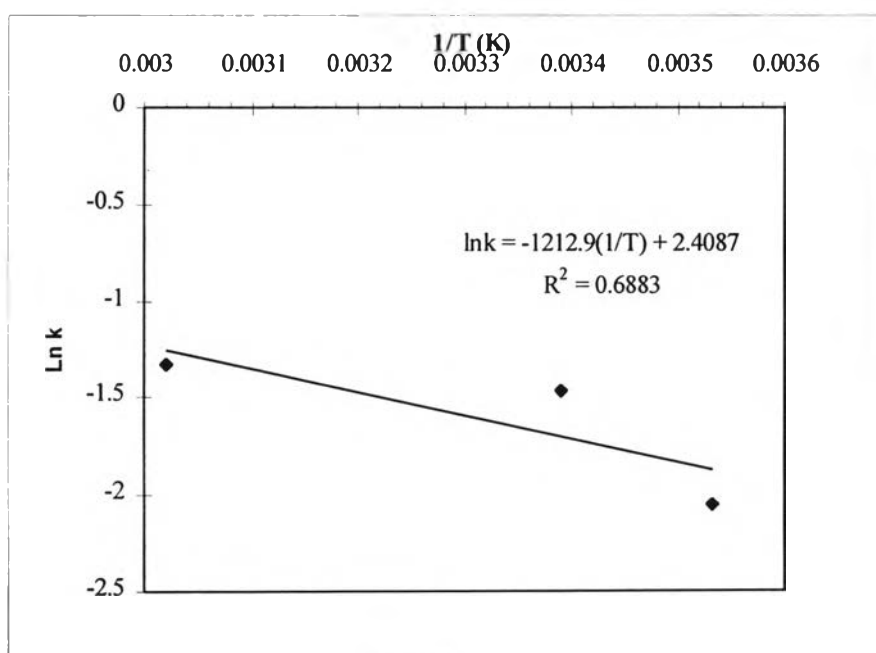


Figure 4.33 The specific dissolution rate constant, k , of asphaltene fraction 2 as a function of the 10wt% DBSA-heptane temperature.

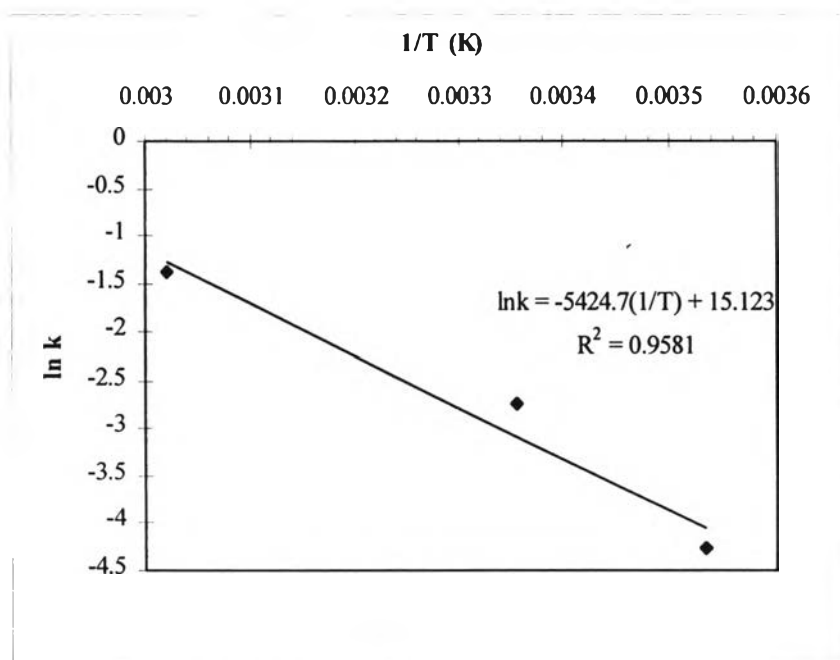


Figure 4.34 The specific dissolution rate constant, k , of asphaltene fraction 1 as a function of the 20wt% NP-heptane temperature.

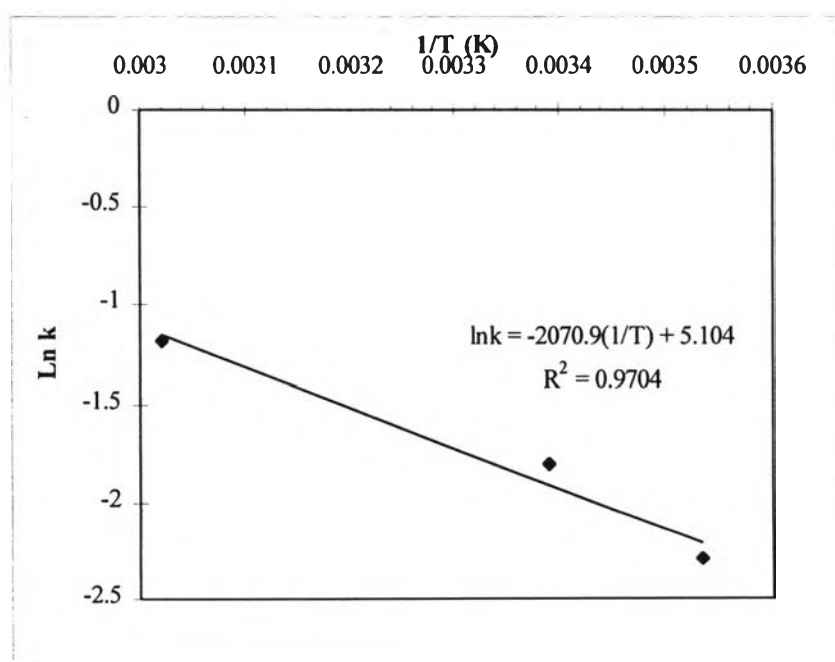


Figure 4.35 The specific dissolution rate constant, k , of asphaltene fraction 2 as a function of the 20wt% NP-heptane temperature.

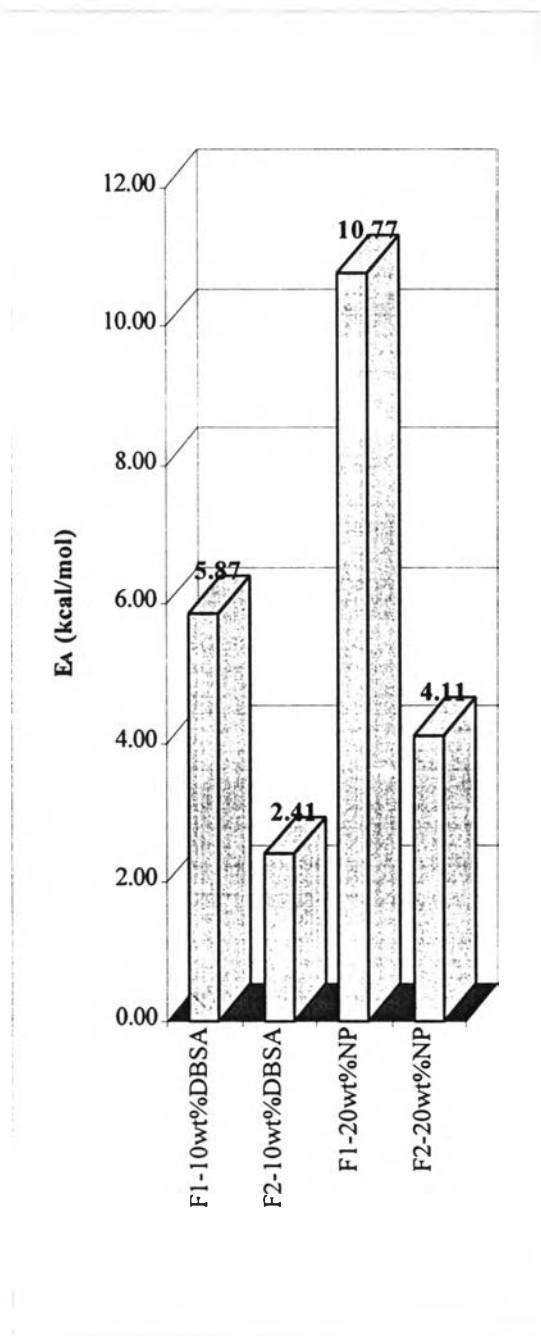


Figure 4.36 The activation energy for dissolution of fractionated asphaltene in the heptane-based fluid containing amphiphiles.